3D Dual-Shell Micro-Resonators for Harsh Environments

Mohammad H. Asadian, Danmeng Wang, Yusheng Wang, Andrei M. Shkel
Department of Mechanical and Aerospace Engineering
University of California, Irvine
Irvine, CA, USA
{asadianm, danmengw, yushengw, andrei.shkel}@uci.edu

***Abstract*—This paper presents the recent advancements in the development of three-dimensional fused quartz dual-shell micro-resonators for environmentally-challenging applications, where the precision measurements are made through shock and vibrations. The dual-shell micro-resonators made from fused quartz and demonstrate a mechanical Q-factor of well above 1 million. An integration and assembly process for capacitive actuation and detection of such resonators using a silicon-in-glass electrode substrate was developed, and electrostatic tuning of n=2 wineglass using out-of-plane electrodes was demonstrated experimentally. We also present a simulation framework based on the Finite Element Method. The modeling approach was used to derive the critical design parameters of the dual-shell micro-gyroscopes for survivability under harsh shock waveforms. The developed 3D dual-shell structure is a potential solution for microresonators and gyroscopes for operation in harsh environments.**

***Index Terms*—Fused Quartz, Resonators, Gyroscopes, 3D MEMS, Environmental Robustness**

I. Introduction

The implementation of Micro-Electro-Mechanical Systems (MEMS) gyroscopes for operation in adverse environmental conditions, such as high-spin rotations, high-g shock, and intense vibrations requires novel structures and designs to maintain the sensors' integrity and enable operation through such harsh conditions. In high-g shock environments, for example, the overall structural and functional integrity of MEMS gyroscopes are affected by the magnitude and duration of the shock. The high mechanical stresses induced by severe shock loads may cause structural failure. The duration of shock defines the major frequency components in the shock waveform, which may excite higher-order vibrational modes in the sensor and magnify the adverse effects on the sensor's overall reliability.

"Non-flat" Coriolis Vibratory Gyroscope (CVG), like Hemispherical Resonator Gyroscope (HRG), provides a rugged structure with higher out-of-plane stiffness as compared to their "flat" counterparts [1]. The in-plane and out-of-plane stiffness in HRG-type devices depends on the 3D geometry of its core sensing element, thus the core hemispherical shell is precisely designed and manufactured to ensure high reliability over its lifetime. In recent years, microfabrication processes based on bulk deformation of fused quartz substrates at high temperature were developed to realize miniaturized, isotropic, and high-Q 3D shell resonators [2]–[4]. The implementation of micro-shell structures to operate as a resonator and a gyroscope, requires an assembly step, at which 3D micro-shells are rigidly bonded to a substrate for capacitive actuation and detection using planar electrodes [5] or peripherally distributed electrodes [6]. In both cases, micro-shells have a single-ended anchor attachment to the substrate through the inner stem. High mechanical shear stress can be induced at the anchor interface because of a limited bonding area, hence anchor attachment becomes the weakest point in assembled sensors. Increasing the bonding area or implementing a double-ended attachment would reduce the anchor stresses and improve structural robustness to high mechanical loads.

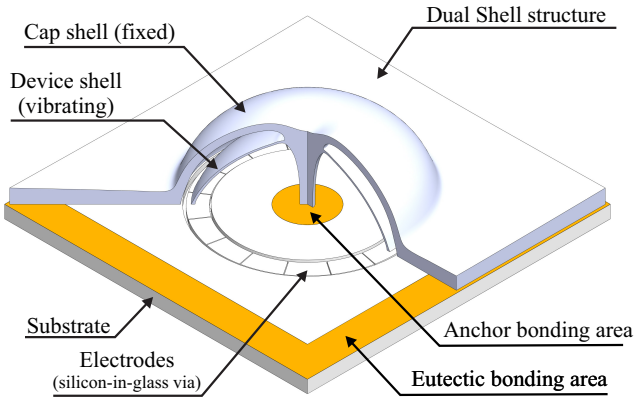

Fig. 1. Schematics of a fused quartz dual-shell micro-resonator. The co-fabricated two-layer shell structure provides (i) a sensing element (device shell), (ii) a self-aligned fixed-fixed double-ended anchor for increased immunity to mechanical shocks and vibrations, and (iii) a housing (cap shell) for vacuum encapsulation.

The 3D fused quartz dual-shell microstructures were introduced in [7], [8], as a core sensing element with a compact form factor which is anticipated to enable a continuous gyro operation through shocks and vibrations. Fig. 1 illustrates schematics of an assembled fused quartz dual-shell gyroscope. The main elements are the dual-shell structure and electrode substrate, which are bonded using eutectic bonding. The fabrication process of dual-shell resonators using micro-

This material is based on work supported by the Defense Advanced Research Projects Agency under Grant N66001-16-1-4021.

978-1-7281-0244-3/20/$31.00 ©2020 IEEE

TABLE I
FREQUENCY RESPONSE DATA OF THE N=2 AND N=3 WINEGLASS MODES OF THE FABRICATED DUAL-SHALL PROTOTYPES.

	n=2 mode			n=3 mode		
Prototype	f (kHz)	df (Hz)	Q-factor	f (kHz)	df (Hz)	Q-factor
#A1	9.671	47.9	262,530	23.263	68.8	1,321,700
#B1	4.905	26.5	945,607	14.581	4.4	1,169,392
#B2	5.499	65.1	1,129,969	16.223	87.6	1,237,700
#B3	4.782	30.9	721,161	13.953	12.7	797,887
#C1	7.914	8.2	313,600	15.638	15.1	1,613,136
#C2	5.456	65.7	1,252,811	15.836	61.6	1,533,332
#C3	6.261	68.2	141,969	16.354	67	862,521
#C4	6.958	30.7	<50,000	19.306	45.1	1,540,475

glassblowing technique was discussed in details in [8]. In the following sections, the recent developments in the design and fabrication of 3D dual-shell devices are reported.

II. CHARACTERIZATION OF DUAL-SHELL RESONATORS

The frequency response of the released and uncoated dual-shell resonator prototypes was characterized using a bulk piezo stack for excitation and a Laser Doppler Vibrometer (LDV) for detection. The piezo stack was attached to the outer shell to excite the resonant modes of the dual-shell structure, and velocity of the inner shell at the rim was captured using LDV. The quality factor of the inner shell was evaluated in a vacuum chamber at <10 μTorr using the amplitude ring-down time measurement. The resonant frequency, frequency mismatch, and the Q-factor of n=2 and n=3 wineglass modes of dual-shell prototypes with different geometries are listed in Table I. The primary sources of frequency mismatch in micro-glassblown shells are a non-uniform heating of the dies inside the furnace, an initial thickness variation across a die before glassblowing, and misalignment in the back-lapping step. The unbalanced mass can be compensated using chemical etching, selective ablation using femtosecond laser, or directional lapping [9].

Fig. 2 shows the results of Q-factor measurements on a dual-shell resonator. We believe the Q-factor of the un-coated shells were limited by surface losses which originated from the quality of the polished surfaces as well as the large surface-to-volume ratio in thin shells and by the residual thermal stresses in the dual-shell resonators which originated from non-isothermal fast cooling after micro-glassblowing.

III. INTEGRATION WITH ELECTRODE SUBSTRATE

An electrostatic capacitive excitation and detection schemes were implemented based on the concept of out-of-plane electrodes for excitation of in-plane wineglass modes [5]. The configuration of electrodes is shown in Fig. 3. An array of 16 planar electrodes provides 4 electrodes for differential actuation (Fx+, Fx-, Fy+, Fy-), 4 electrodes for differential detection (Px+, Px-, Py+, Py-), and 8 electrodes (Q+,Q-) for off-diagonal electrostatic softening and frequency tuning. The electrode substrate provides a connection to bias the resonator through the central stem and a bonding frame for hermetic bonding and vacuum encapsulation of the inner shell.

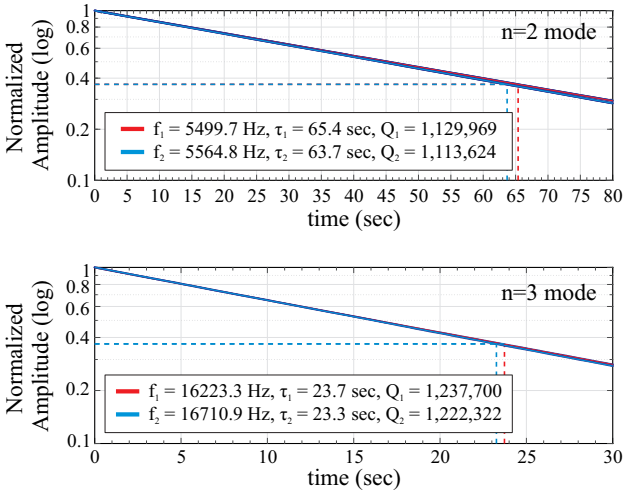

Fig. 2. Experimental Q-factor measurement of a dual-shell prototype (#B2 in Table I) revealed more than 1 minute of ring-down time on n=2 mode.

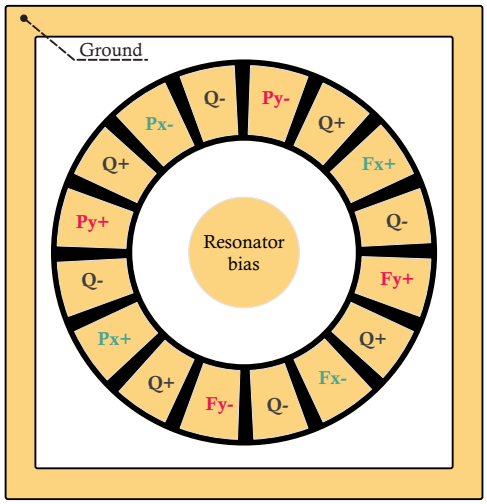

Fig. 3. The electrode configuration for differential excitation and detection of n=2 wineglass modes, green (Fx+, Fx-, Px+, Px-) and red (Fy+, Fy-, Py+, Py-) indicate excitation and detection electrodes for X- and Y-mode, respectively. The Q+ and Q- electrodes are for frequency tuning and mode decoupling.

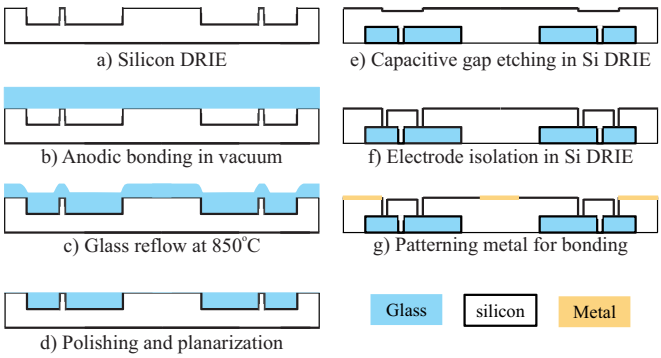

Fig. 4. Fabrication process flow for electrode substrate using silicon-in-glass reflow.

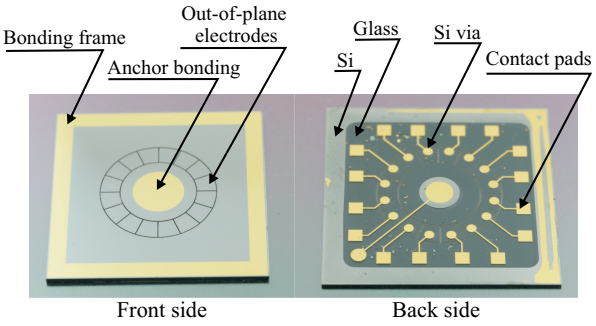

Fig. 5. The front- and back- side of a planar electrode substrate. The eutectic bonding areas (outer frame and anchor) are coated with Cr/Au thin films.

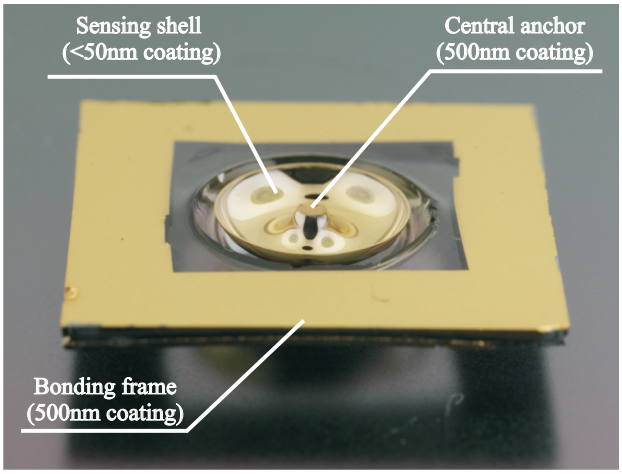

Fig. 6. A metal coated dual-shell prototype (#A1 in Table I) for the electrostatic operation and eutectic bonding.

The electrode substrate was fabricated using the glass-in-silicon reflow process, Fig. 4. Fig. 5 illustrates the front- and back- side of an electrode substrate.

The fused quartz dual-shell was coated for electrostatic operation and eutectic bonding. The device (inner) shell was coated to bias the resonator through the central anchor. A thin conductive coating consisting of 20 nm Cr and 50 nm Au was deposited on the inner shell. The designated areas for the eutectic bonding, such as the bonding frame and the central anchor, were coated with 50 nm Cr and 500 nm Au, Fig. 6.

The eutectic bonding process for assembly with vacuum encapsulation was performed in a SST 3150 furnace. A pre-bake step at 220 $^{\circ}C$ for $>$24 hours was added before the eutectic bonding of the substrate and the dual-shell. This step was performed in order to reduce the out-gassing after vacuum encapsulation. For an active pumping of residual gasses after vacuum sealing, a getter activation is required. This, likely important processing step, was not attempted in this study. The getter material can be deposited in the open area of the silicon substrate in future process iterations. Fig. 7 shows an assembled dual-shell device on the electrode

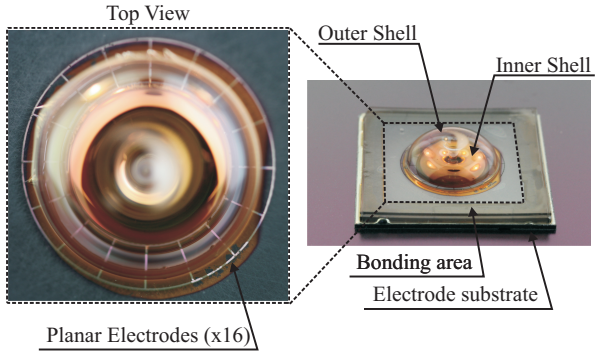

Fig. 7. An assembled fused quartz dual-shell device (#A1 in Table I)).

substrate. The Q-factor of n=2 wineglass mode after assembly and encapsulation was ~219,000. While a reduction in the Q-factor was expected due to metal coating, the measured Q-factor was most-likely limited by air damping. A more effective pre-baking and integration of getter on the electrode substrate would improve the vacuum level and enhance the Q-factor.

IV. Electrostatic Operation

Electrostatic actuation and capacitive detection were implemented with Electromechanical Amplitude Modulation (EAM) technique to eliminate the feed-through parasitics. The AC drive signal of 0.5 Vrms and the DC bias voltage of 5 V were used for the initial frequency response characterization. Fig. 8a shows the electrostatic frequency response of the assembled dual-shell sensor. The fabrication imperfections and misalignment of the wineglass modes with the orientation of electrodes, two peak frequencies appeared in the response plot of each axis, in which the frequency separation between the peaks is equivalent to the frequency mismatch between n=2 wineglass modes. A diagonal and off-diagonal tuning have to be applied for electrostatic tuning of the frequency mismatch. A DC voltage of 63.5 V was applied to the Q+ electrodes for off-diagonal tuning to align the wineglass modes with the drive electrodes, Fig. 8b. For the diagonal tuning, a DC voltage of 47.5 V was applied to the drive electrodes of the Y-axis. A combination of off-diagonal and diagonal tuning voltages reduced the frequency mismatch below 1 Hz (~600 mHz), Fig.8c. The frequency tuning of the dual-shell in-plane wineglass modes was achieved using the planar silicon-in-glass reflow electrodes and the developed assembly process.

V. Design for Robustness to High-g Shock

One of the advantages of the dual-shell structure is an enhanced robustness provided by the additional support through the anchored cap shell. The double-ended anchoring of the device (inner) shell increases the bending stiffness of the stem, thus the resonant modes which are sensitive to in-plane linear acceleration would shift to higher frequencies. The design of the cap anchor radius dramatically influences the stiffness of non-operational modes such as tilt, out-of-plane, rocking,

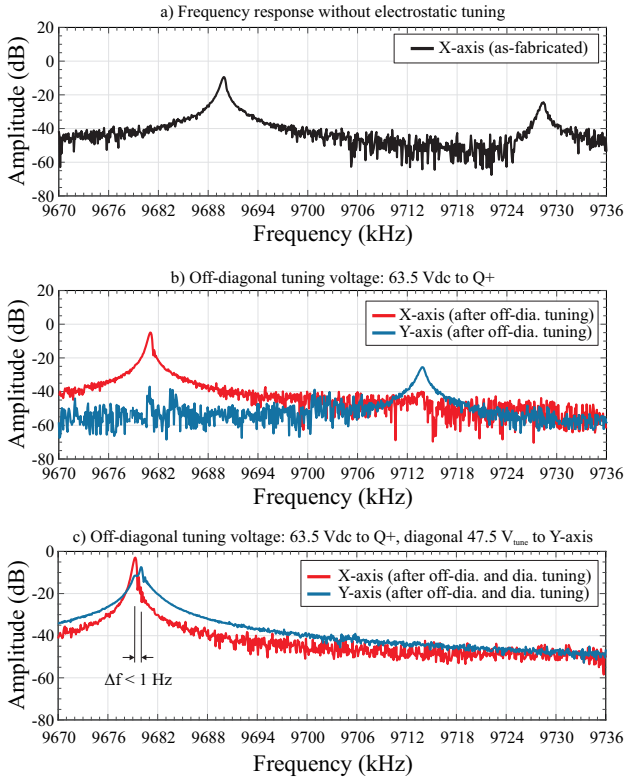

Fig. 8. (a) An electrostatic frequency response characterization of the as-fabricated dual-shell resonator, (b) off-diagonal tuning voltage applied to Q+ electrodes for mode alignment, (c) electrostatic frequency tuning to less than 1 Hz mismatch using off-diagonal and diagonal tuning.

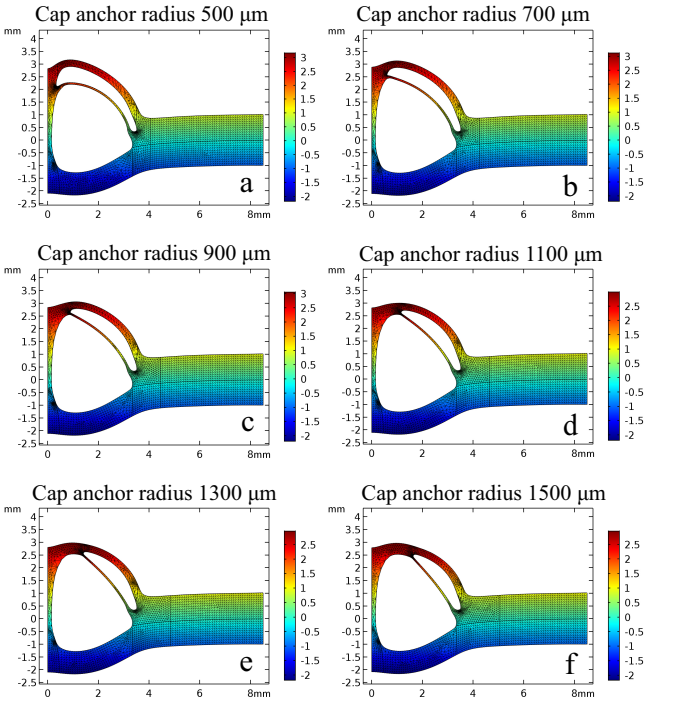

Fig. 9. Parametric finite element results of the dual-shell glassblowing simulations with different cap anchor radius (other geometry parameters are identical).

and rotation modes. For an accurate prediction of the inner shell transient response, a hybrid fluidic-solid finite element model was developed using the COMSOL Multiphysics FE package. Initially, an iso-thermal fluid flow model was utilized to simulate the micro-glassblowing of fused quartz dual-shell resonators and the final geometry of glass-blown structures was predicted. The fluid flow model was discussed in [2], [8]. A 3D solid geometry was constructed by post-processing of the fluid flow simulations results, and used for modal and transient dynamics simulations in a solid mechanics module. A modal superposition technique was utilized to analyze the response of dual-shell devices under mechanical shocks.

Stiffening of the parasitic resonant modes in micro-shells without increasing the frequency of operational modes is challenging [10]. In the dual-shell resonators, the cap anchor size is identified as a critical geometry parameter that can independently stiffen the parasitic modes, hence improve the robustness of micro-shell resonators. As an example, in Fig. 9 the results of glassblowing simulations for different cap anchor radii are demonstrated. The simulations predict that a larger cap anchor radius results in a larger fixed area on top of the device (inner) shell. In these configurations, the n=2 wineglass mode was designed to operate at a relatively low frequency (5 kHz to 20 kHz), while the non-operational modes were shifted to higher frequencies (above 50 kHz). The transient response of dual-shell geometries in Fig. 9 were simulated using the developed finite element simulation framework. An extreme shock load with an amplitude of 50,000g and shock duration of 10 ms was modeled with a half-sine acceleration input and applied to the dual-shell geometries along the in-plane (horizontal) and out-of-plane (vertical) directions. The maximum displacement and maximum principal stress for each case are presented in Table II. The response of a single shell geometry to a similar transient dynamic load was also listed for comparison. The transient dynamics simulation results revealed that the maximum stress will be reduced by an order of magnitude and the maximum displacement was reduced to the sub-micron level, which allows a continuous operation under high shock events without causing a dynamic pull-in instability or physical contact between the sensor and electrode structures.

VI. Conclusions

An integrated 3D fused quartz dual-shell micro-resonator was realized using a micro-glassblowing technique to fabricate the core sensing elements and silicon-in-glass reflow technique to fabricate the electrode substrate. The developed process successfully demonstrated electrostatic excitation, detection, tuning of the device (inner) shell wineglass modes. The dual-shell micro-resonator prototypes with an operational frequency ranging from 5kHz to 10 kHz and as-fabricated frequency mismatch as low as 8.2 Hz with Q-factor of above 1 million were demonstrated. The Q-factor is anticipated to improve

TABLE II
THE TRANSIENT DYNAMIC SIMULATION RESULTS OF THE DUAL-SHELL GEOMETRIES SHOWN IN FIG. 9 UNDER 50,000G SHOCK AMPLITUDE.

	n=2 mode frequency [kHz]	Lowest parasitic mode/frequency [kHz]	Vertical shock max. disp. [μm]	Vertical shock max. stress [MPa]	Horizontal shock max. disp.[μm]	Horizontal shock max. stress [MPa]
Single Shell	12.4	tilt / 9,930	7.4	52.9	21.4	64.3
Case a	10.7	tilt / 9.4	5.3	59.3	30	112
Case b	10.9	tilt / 16.9	0.92	39.5	10.6	110
Case c	14.1	n=3 / 25.5	0.5	16	4.03	52.8
Case d	21.7	n=3 / 25.5	0.36	14.6	1.89	23.6
Case e	32.1	n=3 / 28.1	0.29	14.2	1.1	16.2
Case f	45.4	n=3 / 34.3	0.23	14.2	0.73	14

with higher surface quality and thermal annealing. A finite element simulation framework is developed to predict the transient dynamic response of the dual-shell resonators. The cap shell anchor geometry was identified as the design parameter to improve robustness, which is attributed to selectively stiffening the parasitic resonance modes of the device shell. The developed integration process for electrostatic operation and the simulation framework for robustness improvement are instrumental in the realization of dual-shell microresonators as a rate or rate-integrating gyroscope for continuous operation in harsh environments.

ACKNOWLEDGMENT

The design, modeling, and characterization were performed at UCI Microsystems laboratory. Devices were fabricated at UCI INRF/BiON cleanroom facilities.

REFERENCES

[1] D. M. Rozelle, "The hemispherical resonator gyro: From wineglass to the planets," in *AAS/AIAA Space Flight Mechanics Meeting*, Savannah, Georgia, February, 2009.

[2] M. H. Asadian, Y. Wang, and A. M. Shkel, "Development of 3D Fused Quartz Hemi-Toroidal Shells for High-Q Resonators and Gyroscopes," *IEEE Journal of Microelectromechanical Systems*, vol. 28, no. 6, pp. 954–964, 2019.

[3] D. Senkal, M. J. Ahamed, M. H. Asadian, S. Askari, and A. M. Shkel, "Demonstration of 1 million Q-factor on microglassblown wineglass resonators with out-of-plane electrostatic transduction," *IEEE Journal of Microelectromechanical Systems*, vol. 24, no. 1, pp. 29–37, 2015.

[4] J. Y. Cho, J.-K. Woo, J. Yan, R. L. Peterson, and K. Najafi, "Fused-silica micro birdbath resonator gyroscope," *IEEE Journal of Microelectromechanical Systems*, vol. 23, no. 1, pp. 66–77, 2014.

[5] M. H. Asadian, Y. Wang, S. Askari, and A. M. Shkel, "Controlled capacitive gaps for electrostatic actuation and tuning of 3D fused quartz micro wineglass resonator gyroscope," in *IEEE International Symposium on Inertial Sensors and Systems (INERTIAL)*, Kauai, HI, March 2017.

[6] J. Cho, T. Nagourney, A. Darvishian, and K. Najafi, "Ultra conformal high aspect-ratio small-gap capacitive electrode formation technology for 3d micro shell resonators," in *IEEE 30th International Conference on Micro Electro Mechanical Systems (MEMS)*, Las Vegas, NV, January 2017.

[7] A. M. Shkel, M. H. Asadian Ardakani, and Y. Wang, "Fused quartz dual shell resonator and method of fabrication," 2020, US Application No. 16/836,387.

[8] M. Asadian and A. Shkel, "Fused quartz dual shell resonator," *IEEE International Symposium on Inertial Sensors and Systems (INERTIAL)*, Naples, FL, April 1-5, 2019.

[9] Y. Wang, M. H. Asadian, and A. M. Shkel, "Compensation of frequency split by directional lapping in fused quartz micro wineglass resonators," *Journal of Micromechanics and Microengineering*, vol. 28, no. 9, p. 095001, 2018.

[10] M. H. Asadian, Y. Wang, R. Noor, and A. M. Shkel, "Design space exploration of hemi-toroidal fused quartz shell resonators," in *IEEE International Symposium on Inertial Sensors and Systems (INERTIAL)*, Naples, FL, April, 2019.